ACS APPLIED MATERIALS & INTERFACES

Research Article

www.acsami.org

Porphyrin Sensitizers Bearing a Pyridine-Type Anchoring Group for Dye-Sensitized Solar Cells

Chi-Lun Mai,[†,‡] Thomas Moehl,[‡] Chi-Hung Hsieh,[†] Jean-David Décoppet,[‡] Shaik M. Zakeeruddin,*[,‡] Michael Grätzel,*[,‡] and Chen-Yu Yeh*[,†]

[†]Department of Chemistry and Research Center for Sustainable Energy and Nanotechnology, National Chung Hsing University, Taichung 402, Taiwan

[‡]Laboratory for Photonics and Interfaces, Institute of Chemical Sciences and Engineering, École Polytechnique Fédérale de Lausanne, Lausanne 1015, Switzerland

Supporting Information

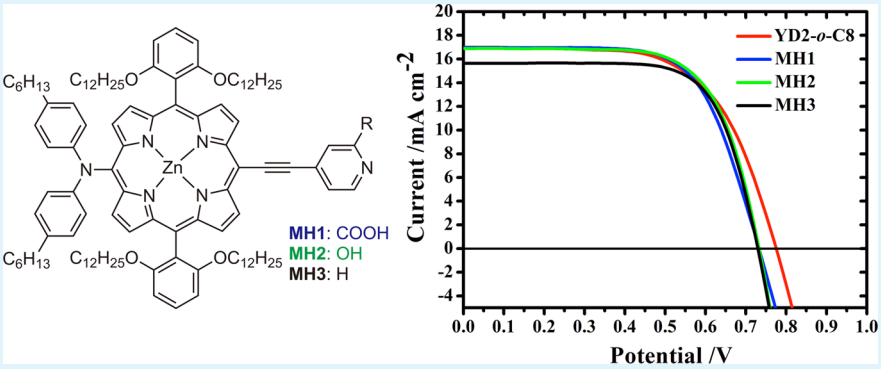

ABSTRACT: Three novel efficient donor−acceptor porphyrins, MH1−MH3, with a pyridine-type acceptor and anchoring group were synthesized and their optical, electrochemical, and photovoltaic properties investigated. Replacing the commonly used 4-carboxyphenyl anchoring group with 2-carboxypyridine, 2-pyridone, and pyridine did not significantly change the absorption and electrochemical properties of the porphyrin dyes. These new porphyrin dyes MH show power conversion efficiencies of 8.3%, 8.5%, and 8.2%, which are comparable to that of the benchmark YD2-*o*-C8 (η = 8.25%) under similar conditions. It was demonstrated that 2-carboxypyridine is an efficient and stable anchoring group as MH1 and showed better cell performance and long-term stability than YD2-*o*-C8 under light soaking conditions.

KEYWORDS: *porphyrin, 2-carboxypyridine, 2-pyridone, pyridine, dye-sensitized solar cell*

1. INTRODUCTION

The development of clean and renewable energy sources reflects the limited fossil resources and severe environmental problems caused by their combustion. Infinite and inexhaustible solar energy is an immense and largely untapped resource to meet a rapidly increasing global energy demand. Dye-sensitized solar cells (DSSCs) have attracted considerable attention since the first report of DSSCs by Grätzel and O'Regan in 1991.[1] DSSCs may become a potential alternative to conventional silicon-based solar cells because of their high light-to-electricity conversion efficiencies, ease of fabrication, colorful and decorative nature, and low production costs. The most widely used sensitizers for DSSCs are based on ruthenium complexes due to their broad absorption in the visible and/or near IR region, high efficiency, and long-term stability. The devices of ruthenium dyes have achieved power conversion efficiency (PCE) of more than 11%.[2,3] However, the potential environmental concern, limited availability, and cost of ruthenium metal might hinder their wide application.

In the past two decades, many efforts have been devoted to the development of organic sensitizers that are suitable for practical use. Some organic dyes have achieved an impressive PCE of over 10%.[4−7] Such efficient organic dyes share a common D-π-A structure that broadens the absorption in the visible region and has appropriate electron distribution for the HOMO and LUMO, facilitating charge separation and decreasing charge recombination. A variety of moieties such as triphenylamine,[8−11] aniline,[12,13] indoline,[14,15] carbazole,[16−19] fluorine,[20] cyanine,[21−23] coumarin,[19,24−26] and phenothiazine[20,27−30] have been employed as the donors in D-π-A dyes. Unlike many options for the donor, electron-deficient components such as carboxylic acid, cyanoacrylic acid, and rhodanine-3-acetic acid were generally introduced to the dyes as the acceptor and anchoring group. Among these anchors, cyanoacrylic acid is the most commonly used acceptor and

Received: May 4, 2015
Accepted: June 17, 2015
Published: June 17, 2015

ACS Publications © 2015 American Chemical Society

DOI: 10.1021/acsami.5b03783
ACS Appl. Mater. Interfaces 2015, 7, 14975−14982

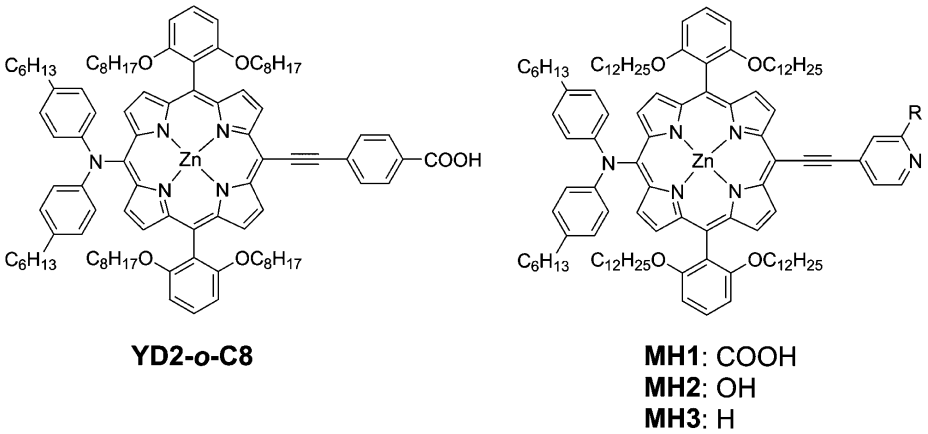

Figure 1. Molecular structures of the (left) YD2-*o*-C8 and (right) MH1, MH2, and MH3 porphyrin dyes.

anchoring group because it red shifts and broadens the absorption spectra and shows better electron injection efficiency. However, the use of cyanoacrylic acid as the binding unit results in degradation of dyes from the TiO_2 surface under long-term irradiation.[31] In addition, such an anchor undergoes trans-to-cis photoisomerization, which competes with electron injection and is deleterious to the cell performance of the dyes.[32] Therefore, electron-withdrawing groups such as pyridine,[33,34] phosphinic acid,[35] 8-hydroxyquinoline,[36] pyridinium,[37,38] and 2-(1,1-dicyanomethylene)rhodanine[39] have been tested as the anchoring moiety. Recently, Ooyama and co-workers reported the use of pyridine as an acceptor and anchor of carbazole-based organic dyes and found that the pyridine coordinated to the Lewis acid sites of TiO_2, giving efficient electron injection due to good electronic communication between the pyridine and Ti atom.[33,34,40,41] However, dye loading for sensitizers with pyridine anchor is lower than those of carboxylic acid analogues. Calamante et al. designed and synthesized an organic dye featuring a pyridine-*N*-oxide 2-carboxylic acid as an acceptor and anchoring group, of which contemporary presence of *N*-oxide and carboxylic acid resulted in robust binding of the dye to the TiO_2 surface and was able to enhance the stability of the dye.[42] Sun et al. employed *N*-(carboxymethyl)pyridinium as an electron-withdrawing anchoring group for a series of hemicyanine dyes, which showed much higher PCE than the cyanoacrylic acid counterparts. The best performing dye achieved an efficiency of 7.0%.[37]

Porphyrins are one of the most studied molecules because they are wide-spread in natural systems and perform a variety of biological activities such as dioxygen transport and storage, and catalytic oxidation of organic substrates. Inspired by the pivotal role chlorophylls play in energy and electron transfer processes in the active site of photosynthetic plants and bacteria, porphyrins have been recently considered as potential and promising candidates for highly efficient DSSCs. The use of porphyrins in DSSCs has several advantages: (1) their intense absorption in Soret and Q bands efficiently harvests solar energy in a broad spectral region; (2) there are four meso- and eight β-positions for facile molecular modification; (3) they show unique photophysical and electrochemical properties that can be fine-tuned in a controllable fashion. In recent years, a number of highly efficient porphyrins with PCE of over 10% have been developed.[43−46] The best performing porphyrin dyes have achieved a PCE higher than 12% for DSSCs in combination with cobalt electrolyte.[47−49]

We describe herein the synthesis, and the optical, electrochemical, and photovoltaic properties of push−pull porphyrins MH1, MH2, and MH3 with pyridyl-type as the acceptor and anchoring groups in which 2-pyridinecarboxylic acid and 2-pyridone anchors were incorporated for the first time into sensitizers for DSSCs. Previous studies showed that the cell performance for porphyrin dyes with an anchoring group other than benzoic acid or cyanoacrylic acid is generally poor. In this study, the devices of MH1−MH3 used in conjunction with liquid I^-/I_3^- redox electrolyte exhibited excellent cell performance and remarkable stability under long-term irradiation, which are comparable or slightly better than the benchmark YD2-*o*-C8 porphyrin dye, indicating that 2-carboxypyridine and 2-pyridone are promising candidates as an effective acceptor and anchoring group. The MH1 and MH2 achieved an efficiency of 8.3% with J_{SC}/mA cm^{-2} = 16.85, V_{OC}/mV= 738, FF = 0.67 and 8.5% with J_{SC}/mA cm^{-2} = 16.88, V_{OC}/mV= 735, FF = 0.682, respectively. To the best of our knowledge, the MH1- and MH2-based devices in combination with I^-/I_3^- electrolyte show the highest PCEs for organic dyes containing an anchoring group other than commonly used benzoic acid or cyanoacrylic acid.

2. RESULTS AND DISCUSSION

2.1. Absorption and Electrochemical Properties. A series of porphyrin dyes with 2-carboxypyridine, 2-pyridone, and pyridine group as the electron acceptor and anchoring group replacing the traditional anchoring groups, such as the carboxyl group have been synthesized and used in dye-sensitized solar cells (Figure 1).[49] The porphyrin dyes were based on the molecular structure of our previously developed D-π-A dye YD2-*o*-C8 with the donor attached at the meso-position of the porphyrin core opposite to the acceptor at the meso-position. The detailed synthetic procedures are described in the Supporting Information.

Figure 2 shows the UV/vis absorption spectra of MH1, MH2, and MH3 in THF with the features typical of a porphyrin ring, consisting of an intense Soret band in the range of 400−500 nm and less intense Q bands in a range from 550 to 700 nm. The molar absorption coefficients/10^5 M^{-1} cm^{-1} for the Soret band of these porphyrin dyes range from 1.70 to 2.18, whereas those/10^3 M^{-1}cm^{-1} of the Q bands are in the range 28.6 to 31.7 and the data are listed in Table 1. In a comparison of the absorption spectra, MH2 and MH3 show

DOI: 10.1021/acsami.5b03783
ACS Appl. Mater. Interfaces 2015, 7, 14975−14982

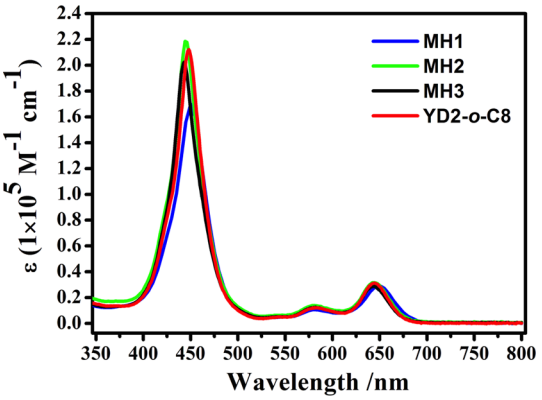

Figure 2. UV−visible absorption spectra of the YD2-*o*-C8, MH1, MH2, and MH3 sensitizers in THF.

slight blue shift absorption whereas MH1 exhibits red shifted absorption for both the Soret and Q bands.

The electrochemical properties of porphyrins MH1−MH3 were investigated by cyclic voltammetry in dry acetonitrile with tetrahydrofuran (3:1 v/v) containing 0.1 M $TBAPF_6$ as the supporting electrolyte (Figure S1 in the Supporting Information).Because of limited dyes solubility, we applied solvent mixture for cyclic voltammetry. The HOMO energy levels of MH1−MH3 were determined by the first oxidation potentials (E_{ox}), which were observed at +0.84, +0.84, and +0.85 V against the normal hydrogen electrode for MH1, MH2, and MH3, respectively. Even though we used a solvent mixture, we took 0.63 V normally used for pure acetonitrile as a conversion factor to convert ferrocene/ferrocenium to NHE values. The HOMO levels of MH1, MH2, and MH3 are negatively shifted by 40, 10, and 30 mV, respectively, compared to that of YD2-*o*-C8 due to the electron withdrawing nature of the pyridyl acceptors.

The HOMOs of all these porphyrin dye are more positive than the oxidation potential for I^-/I_3^- redox couple (+0.40 V vs NHE),[51,52] which meets the requirement for effective dye regeneration by electron transfer from I^- to the oxidized dye.[53] The energy levels of the first excited states were calculated by the equation, $E^*_{0-0} = E_{ox1} - E_{0-0}$, in which E_{ox1} is the first oxidation potential of the dye and E_{0-0} is the zero−zero excitation energy determined from the intersection of the corresponding absorption and emission spectra.[53,54] The E^*_{0-0} values of MH1, MH2, and MH3 were calculated to be −1.04, −1.06, and −1.05 V, respectively, which are more negative than the conduction edge (−0.50 V vs NHE) of TiO_2,[52] providing sufficient driving force for electron injection from the photoexcited sensitizers to the conduction band (CB) of TiO_2 (Figure 3).

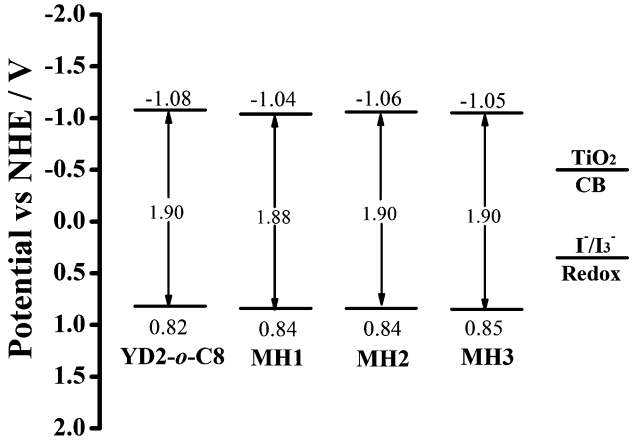

Figure 3. Schematic energy levels of YD2-*o*-C8, MH1, MH2, and MH3 based on electrochemical, absorption, and emission data.

2.2. DFT Calculation. To gain understanding of the molecular geometries and electron distribution of the frontier and nearby molecular orbitals, we performed quantum-chemical calculations on porphyrins MH1−MH3 using density functional theory (DFT) at the B3LYP/6-31G(d) level (Spartan 08 package). To simplify the computations, some alkyl groups on phenyl rings were replaced with hydrogen atoms or methyl groups. The electron density of HOMOs is delocalized over the π system of the porphyrin ring, the diarylamine moiety and the phenylethyne (PE) linker, whereas the LUMOs are distributed on the porphyrin ring and anchoring group (Figure S2 in the Supporting Information). The presence of a carboxyl group at the pyridyl of MH1 increases the electron density of the pyridyl ring as compared to those of MH2 and MH3. This would influence the electronic coupling between the excited adsorbed dye and the 3d orbitals of TiO_2.[55] The HOMO-1 and LUMO +1 show electron density solely located on the porphyrin ring.

2.3. Binding Mode of the Anchoring Group to the TiO_2 Surface. To understand better the adsorption properties of porphyrin dyes MH1−MH3, we also investigated their FTIR spectra of the dye powders and the dyes adsorbed on TiO_2 film (Figure 4). When the molecules of MH1 are bound to TiO_2, the carboxylate at 1637 cm^{-1} disappeared and no ester-type bonding was observed; the possible structure is that both oxygen atoms are bound to TiO_2. The band at 1642 shifted to 1633 cm^{-1} as the molecules of MH2 were bound to TiO_2, the

Table 1. Spectral, Electrochemical and Photovoltaic Properties of YD2-*o*-C8, MH1, MH2, and MH3

dye	λ_{abs} (cm^{-1}) (log ε)[a] neutral form	emission[b] λ_{max} (nm)	oxidation[c] $E_{1/2}$ (V) (vs NHE)	E_{0-0} (V) (vs NHE)	E^*_{0-0} (V) (vs NHE)	DL[d] nmol cm^{-2}
YD2-*o*-C8	448(212), 582(12), 645(31)	663	+0.82	1.90	−1.08	55
MH1	450(170), 580(11), 650(29)	673	+0.84	1.88	−1.04	115
MH2	445(218), 580(14), 643(32)	666	+0.84	1.90	−1.06	21
MH3	442(202), 581(12.4), 643(31)	664	+0.85	1.90	−1.05	7.2

[a]Absorption and emission data were measured in THF at 25 °C. [b]The excitation wavelengths were 663, 673, 666, and 664 nm for YD2-*o*-C8, MH1, MH2, and MH3, respectively. [c]Electrochemical measurements were performed at 25 °C for MH1−MH3 in THF/ACN (1:3 v/v) containing $TBAPF_6$ (0.1 M) as supporting electrolyte. Potentials were reported versus NHE and reference to the ferrocene/ferrocenium (Fc/Fc^+) couple by addition of 630 mV. [d]The amounts of dye loading, indicated as YD2-*o*-C8, MH1, MH2, and MH3, were determined from the desorption of dye molecules on immersion of transparent 4 μm TiO_2 electrodes in a basic solution of 0.05 M tetrabutylammonium hydroxide in EtOH and the calibrated absorption.

DOI: 10.1021/acsami.5b03783
ACS Appl. Mater. Interfaces 2015, 7, 14975−14982

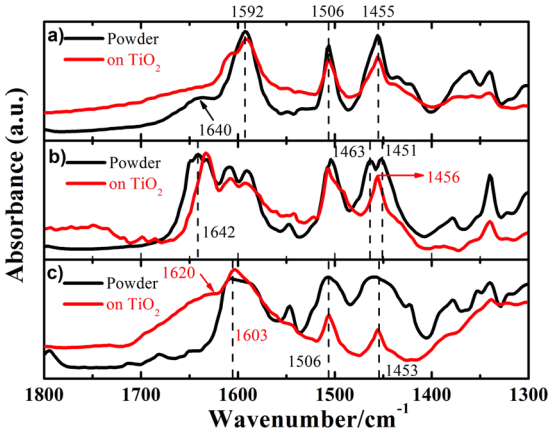

Figure 4. FTIR spectra of dye powders (black lines) and dyes adsorbed on TiO_2 nanoparticles (red lines) for (a) MH1, (b) MH2, and (c) MH3.

bands at 1463 and 1452 disappeared, and a new band at 1456 cm^{-1} was observed. Most likely both nitrogen and oxygen atoms are coordinated to the Lewis acid site of TiO_2, i.e., surface titanium ions. A new broad band at around 1630 cm^{-1} was observed as MH3 adsorbed on TiO_2, which can be assigned to the pyridyl coordinated group to the Lewis acid sites on the TiO_2 surface. The band at 1608 cm^{-1} slightly shifted to 1603 cm^{-1}, which can be ascribed to hydrogen bonding of nitrogen to the Brønsted acid sites of the surface of TiO_2 (Figure 5).[33,34,40,41]

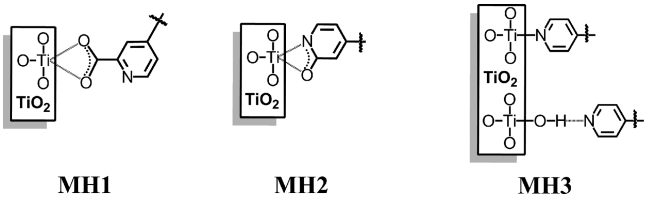

Figure 5. Coordination of the MH1, MH2, and MH3 on the TiO_2 surface.

2.4. Photovoltaic Characteristics. Figure 6 shows current−voltage (J−V) characteristics curves for DSSCs based on porphyrins MH1, MH2, and MH3 under simulated AM 1.5 G irradiation. The photovoltaic parameters are summarized in Table 2. The devices consist of a double layer TiO_2 film with

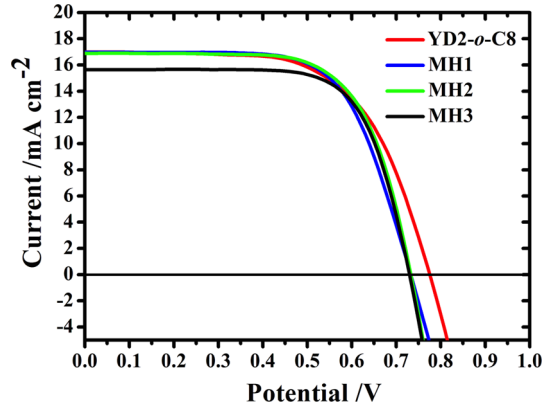

Figure 6. I−V characteristics of the devices made with YD2-*o*-C8, MH1, MH2, and MH3 (with 0.4 mM CDCA) dyes used I^-/I_3^- based redox electrolyte.

Table 2. Photovoltaic Characteristics for DSSCs Based on MH1, MH2, and MH3 Using THF:EtOH (1:4) as Sensitizing Bath Solvent and Z960 (volatile) as Electrolyte

dye	power (mW/cm^2)	Jsc (mW/cm^2)	V_{oc} (mV)	FF	PCE (%)
YD2-*o*-C8	97.7	16.97	779	0.625	8.25
MH1	98.6	16.85	738	0.670	8.3
MH2	99.2	16.88	735	0.682	8.5
MH3	96.9	15.60	731	0.718	8.2

porphyrin dye adsorbed on the surface by dipping the TiO_2 film in a dye solution of THF−EtOH (1:4, v/v) for 12 h, a platinum-coated glass as the counter electrode, and a solution of 1.0 M 1,3-dimethylimidazolium iodide (DMII), 0.03 M I_2, 0.1 M guanidinium thiocyanate, 0.5 M TBP, and 0.05 M LiI in a mixture of acetonitrile−valeronitrile (85:15, v/v) as the redox electrolyte (labeled as Z960). Under optimized conditions, the devices exhibit high J_{SC} values of 16.85 mA cm^{-2} for MH1 and 16.88 mA cm^{-2} for MH2, which are comparable to that of YD2-*o*-C8 (J_{SC} = 16.97 mA cm^{-2}). For MH3, 15.6 mA cm^{-2} was obtained and the obtained lower photocurrent can be explained due to low dye-loading (Table 2). The photovoltages of these three porphyrins are lower than that of the reference YD2-*o*-C8. The decreased photovoltage can be explained by the electrochemical impedance results that will be discussed later. Under similar conditions, MH1 and MH2 showed excellent cell performance, exceeding that of YD2-*o*-C8, indicating 2-carboxypyridine and 2-pyridone to be good anchors for the prophyrins. The devices achieved an efficiency of 8.3% with J_{SC}/mA cm^{-2} = 16.85, V_{OC}/mV = 738, FF = 0.670 for MH1, and 8.5% with J_{SC}/mA cm^{-2} = 16.88, V_{OC}/mV = 735, FF = 0.682 for MH2. As shown in Figure 5, these dyes exhibit broad IPCE (the efficiencies of conversion of incident photons to current responses) in the visible region with high IPCE values of around 70−90% at regions of 400−500 and 600−700 nm were observed (Figure 7).

2.5. Electrochemical Impedance Spectroscopy. Taking a look at the dark current of the devices (Figure 8a) with the different sensitizers, one can observe similar behavior for the three new dyes while the dark current of the YD2-*o*-C8 device is lower at higher forward bias. This difference originates normally either from a different conduction band position of

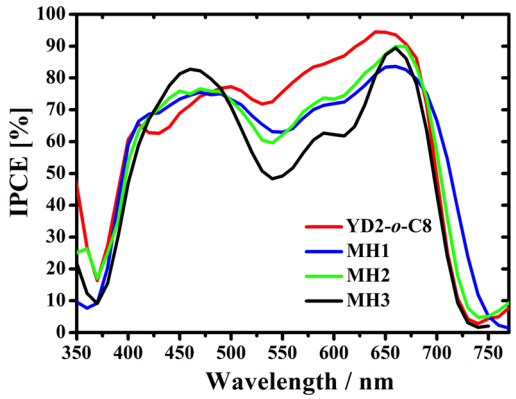

Figure 7. Photocurrent action spectrum (IPCE) of the same devices made with YD2-*o*-C8, MH1, MH2, and MH3 (with 0.4 mM CDCA).

DOI: 10.1021/acsami.5b03783
ACS Appl. Mater. Interfaces 2015, 7, 14975−14982

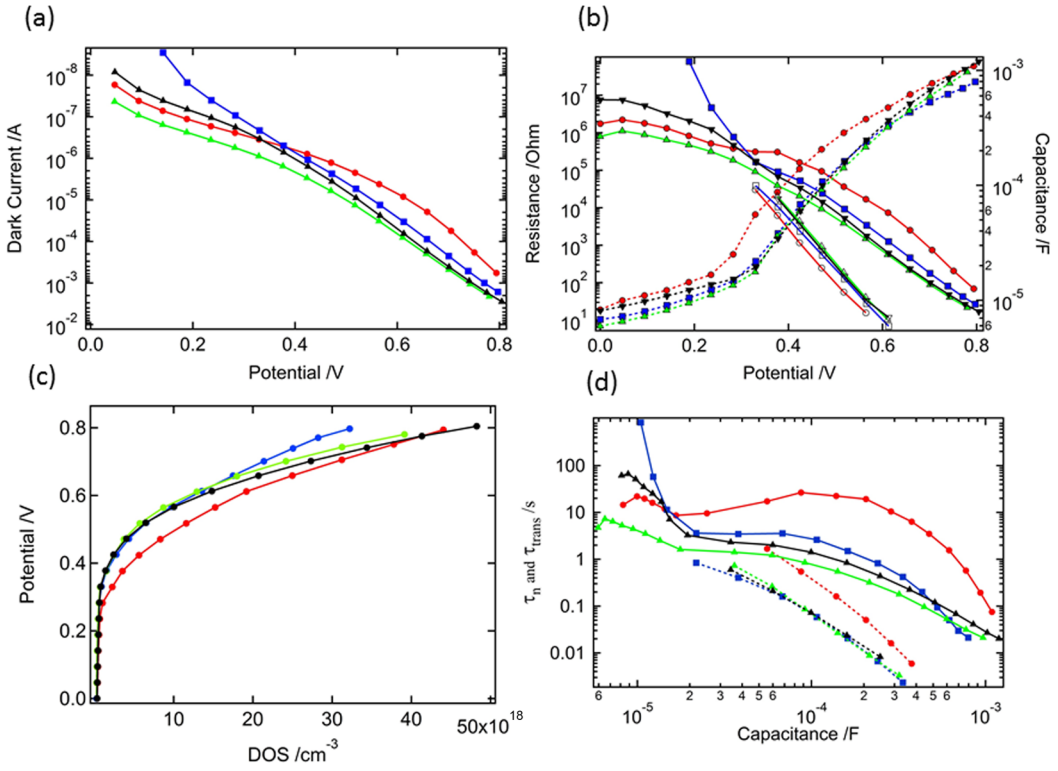

Figure 8. (a) Dark current of the different devices during the EIS measurement. YD2-*o*-C8, red; MH1, blue; MH2, green; MH3, black; (b) R_{ct} (full markers, solid line), R_{trans} (empty markers, solid line), and C_μ (full markers, dotted line) extracted from the EIS measurements; (c) comparison of the DOS of the devices made with the different dyes; (d) τ_n (solid) and τ_{trans} (dotted line) calculated from the EIS results plotted against the chemical capacitance. The potential is corrected for the IR drop.

the mesoporous metal oxide or from a change in recombination at the mesoporous metal oxide/electrolyte interface or from a combination of the two effects.

To understand in more detail the cause or the causes for the different V_{oc}, we have performed electrochemical impedance measurements (EIS). EIS analysis can reveal a shift in the chemical capacitance of the TiO_2 due to a movement of the TiO_2 conduction band (E_{CB}) and also change in the charge transfer resistance if recombination is the major reason for the observed differences in V_{oc}.

The main results from the fitting procedure of the impedance spectra are presented in Figure 8b showing the charge transfer resistance representing the resistance for the recombination of the TiO_2 conduction band electrons with the oxidized redox species in the electrolyte, R_{ct}, the transport resistance for the electrons inside the mesoporous metal oxide, R_{trans}, and chemical capacitance representing the filling of the traps inside the mesoporous TiO_2, C_μ.

Plotting the IR-drop corrected potential vs the DOS (Figure 8c, with the DOS equal to $C_\mu/qAL(1-p)$ with q the electron charge, A the geometric area of the cell, L the thickness of TiO_2, and p the film porosity), the change in conduction band position can be estimated. One has to keep in mind that for the comparison of the conduction band position of the TiO_2 in the devices, the change in the shape of the DOS should be small. Toward higher chemical capacitances, a deviation of the shape between YD2-*o*-C8 and MH1 on one side and the MH2 and MH3 on the other side can be observed. Because the dyes MH2 and MH3 have the nitrogen directly involved in the binding mechanism to the metal oxide surface, this might be a reason for the different shape of the DOS toward higher voltage.

In contrast the devices with YD2-*o*-C8 and MH1 where the binding mechanism is over a carboxylate anchoring group show a very similar shape of C_μ over the whole potential range but a lower conduction band of the TiO_2 for the devices with YD2-*o*-C8. Estimating the difference in conduction band position over the DOS at about 2×10^{19} (with YD2-*o*-C8 as the reference point) for MH1, MH2, and MH3 yields ~50 to 60 mV. As mentioned, at higher forward biases the shape of the DOS is changing in the cases of the MH2 and MH3. Therefore, the estimation for these two dyes has to be taken with great care.

One can use the DOS or the chemical capacitance as a reference and compare the different electron lifetimes at a similar charge density canceling out the difference in E_{CB} position (Figure 8d). At a capacitance of about 0.6×10^{-3} F the electron lifetimes are about 30 times higher for YD2-*o*-C8. Using the diode equation and assuming a value of one for the diode ideality factor, this would lead to an increase in the V_{oc} of about 88 mV for YD2-*o*-C8 compared to the other dyes. Taking into account the observed downward shift in the DOS of 50 to 60 mV, the net gain in V_{oc} would be about 28 to 38 mV. A similar protocol can be applied by comparing the change in electron lifetime in relation to the conductivity of the metal oxide (Figure 9). Both approaches yield similar changes in the V_{oc} that are close to the observed difference of 35 to 40 mV. The above analysis shows that the MH family distinguishes itself clearly from YD2-*o*-C8 manifesting different binding patterns and introducing changes in the conduction band position of the TiO_2, the shape of the DOS, and of the electron transport as well as recombination time.

DOI: 10.1021/acsami.5b03783
ACS Appl. Mater. Interfaces 2015, 7, 14975−14982

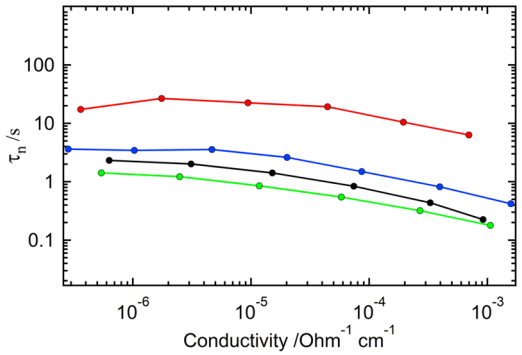

Figure 9. Comparison of the electron lifetime against the conductivity of the TiO_2.

As mentioned, one can try to estimate the change in E_{CB} by the shift in R_{trans}. R_{trans} should be dependent on the amount of electrons inside the E_{CB} of the TiO_2 thermalized from the DOS. Interestingly, the change in R_{trans} between YD2-*o*-C8 and the MH dyes is only about 30 mV. Determining the reasons for this effect are beyond the scope of this publication, but explanations can be, e.g., how the dyes organize on the TiO_2 surface, the ionic reorganization at the interface metal oxide and electrolyte and the interaction of the different anchoring group with the metal oxide surface.

The electron transport is also strongly influenced by the dye structure when changing from YD2-*o*-C8 to the MH dye series. This can be observed in Figure 8b,d. The electron transport and lifetime can be calculated from the product of the chemical capacitance and transport resistance and the recombination resistance, respectively. Clearly, the electron transport and lifetime are very similar for the MH dyes. In contrast, the electron transport and lifetime are higher for the YD2-*o*-C8 dye at a similar charge density inside the TiO_2 (which was already implied by the difference in the shift of the DOS and the transport resistance). One way to circumvent the problem of the comparison of electron lifetime at similar charge density is to plot the electron lifetime against the conductivity of the TiO_2 (see Figure 9). In this case, the comparison is only over a short part of the applied potential range (because the transport resistance can only be determined up to about 600 mV).

Using the conductivity as relation, one yields about 10 times higher lifetime for the YD2-*o*-C8 dye compared to the other tree dyes. This leads to a higher voltage of about 60 mV by longer electron lifetime for YD2-*o*-C8. Subtracting the 30 mV from the difference between the transport resistance of the MH dyes and the YD2-*o*-C8 leads to about 30 mV higher V_{oc} for the devices with YD2-*o*-C8.

2.6. Long-Term Stability. Figure 10 shows the photovoltaic performance during long-term accelerated aging of MH-sensitized solar cells using an ionic-liquid based electrolyte under simulated AM 1.5 G (100 mW cm^{-2}) at 60 °C. The photovoltaic parameters were recorded over a period of 1000 h. In these solvent-free ionic-liquid devices, MH1 and MH2 showed initial power conversion efficiencies (PCEs) of 7.2% and 5.9%, respectively, whereas the PCE of YD2-*o*-C8 was 6.2%. The devices of MH1, MH2, and YD2-*o*-C8 maintained around 90%, 69%, and 85%, respectively, of their initial efficiencies after 1000 h of light-soaking, indicating that 2-carboxypyridyl is superior to 4-carboxyphenyl as an anchoring group in terms of the power conversion efficiency and long-term stability of the dyes.

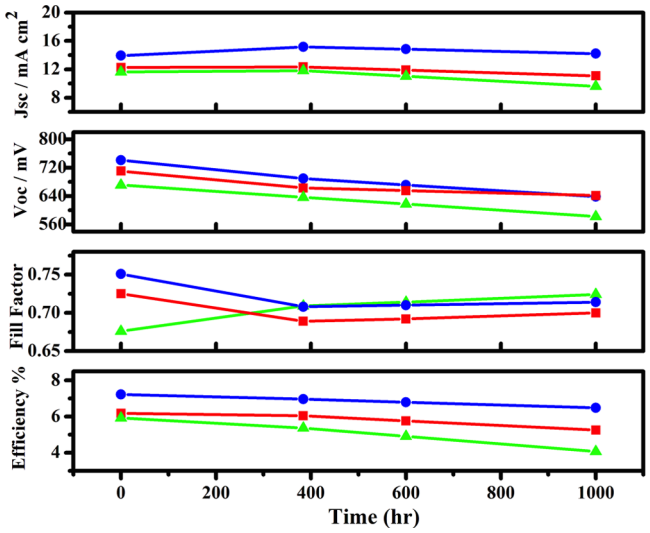

Figure 10. Stability test illustrating photovoltaic parameter (Jsc, V_{oc}, FF, and η) variations with aging time for the devices based on YD2-*o*-C8 (red square), MH1 (blue circle), and MH2 (green triangle)-sensitized TiO_2 films with a solvent-free ionic-liquid electrolyte during 1 sun visible light irradiation at 60 °C.

3. CONCLUSION

In summary, we have successfully designed and synthesized a series of new D-π-A porphyrin sensitizers with pyridyl anchoring groups, and demonstrated that the 2-carboxylpyridine, 2-pyridone, and pyridine anchoring groups strongly bind to the Lewis acid sites formed by coordinatively unsaturated Ti(IV) ions at the TiO_2 surface. The devices based on the MH1, MH2, and MH3 showed good photovoltaic performance, comparable to that of the standard YD2-*o*-C8 sensitizer. Devices fabricated with ionic-liquid based electrolyte retained 90% and 85% of their initial efficiencies for MH1 and YD2-*o*-C8, respectively, after 1000 h of light soaking at 60 °C, indicating the significance of the anchoring group in promoting long-term stability of DSSCs. With respect to the power conversion efficiency and long-term stability of the devices, 2-carboxypyridyl outperforms the 4-carboxyphenyl as the anchoring group and acceptor. We are now trying to incorporate these promising alternative anchoring groups into organic dyes to replace commonly used cyanoacrylic acid and carboxyl groups.

■ ASSOCIATED CONTENT

Supporting Information

General synthetic procedures; HOMO and LUMO characteristics; cyclic voltammogram for complexes YD2-*o*-C8, MH1, MH2, and MH3. The Supporting Information is available free of charge on the ACS Publications website at DOI: 10.1021/acsami.5b03783.

■ AUTHOR INFORMATION

Corresponding Authors

*S. M. Zakeeruddin. E-mail: shaik.zakeer@epfl.ch.
*M. Grätzel. E-mail: michael.graetzel@epfl.ch.
*C.-Y. Yeh. E-mail: cyyeh@dragon.nchu.edu.tw.

Author Contributions

C.-L.M. performed the photovoltaic measurements, optimized DSC devices, synthesized dyes and wrote the paper. T.M. analyzed the electrochemical impedance data and wrote the

DOI: 10.1021/acsami.5b03783
ACS Appl. Mater. Interfaces 2015, 7, 14975−14982

manuscript. C.-H.H. synthesized dyes and characterized. J.-D.D. performed the photovoltaic for long-term stability measurements. C.-Y.Y. designed dye structures supervised all the synthetic work and wrote the manuscript. S.M.Z. and M.G. designed and supervised the photovoltaic experiments, analyzed the results and wrote the paper.

Notes

The authors declare no competing financial interest.

■ ACKNOWLEDGMENTS

C.-Y.Y. is grateful for the financial support of the Ministry of Science and Technology of Taiwan and the Ministry of Education of Taiwan. M.G. thanks the Swiss National Science Foundation and CTI 17622.1 PFNM-NM grant, glass2-energy SA (g2e), Villaz-St-Pierre, Switzerland for financial support.

■ REFERENCES

(1) O'Regan, B.; Grätzel, M. A Low-Cost, High-Efficiency Solar Cell Based on Dye-Sensitized Colloidal TiO_2 Films. *Nature* **1991**, *353*, 737−740.

(2) Gao, F.; Wang, Y.; Shi, D.; Zhang, J.; Wang, M.; Jing, X.; Humphry-Baker, R.; Wang, P.; Zakeeruddin, S. M.; Grätzel, M. Enhance the Optical Absorptivity of Nanocrystalline TiO_2 Film with High Molar Extinction Coefficient Ruthenium Sensitizers for High Performance Dye-Sensitized Solar Cells. *J. Am. Chem. Soc.* **2008**, *130*, 10720−10728.

(3) Yu, Q.; Wang, Y.; Yi, Z.; Zu, N.; Zhang, J.; Zhang, M.; Wang, P. High-Efficiency Dye-Sensitized Solar Cells: The Influence of Lithium Ions on Exciton Dissociation, Charge Recombination, And Surface States. *ACS Nano* **2010**, *4*, 6032−6038.

(4) Yang, J.; Ganesan, P.; Teuscher, J.; Moehl, T.; Kim, Y. J.; Yi, C.; Comte, P.; Pei, K.; Holcombe, T. W.; Nazeeruddin, M. K.; Hua, J.; Zakeeruddin, S. M.; Tian, H.; Grätzel, M. Influence of the Donor Size in D-π-A Organic Dyes for Dye-Sensitized Solar Cells. *J. Am. Chem. Soc.* **2014**, *136*, 5722−5730.

(5) Zhu, W.; Wu, Y.; Wang, S.; Li, W.; Li, X.; Chen, J.; Wang, Z.-S.; Tian, H. Organic D-A-π-A Solar Cell Sensitizers with Improved Stability and Spectral Response. *Adv. Funct. Mater.* **2011**, *21*, 756−763.

(6) Zeng, W.; Cao, Y.; Bai, Y.; Wang, Y.; Shi, Y.; Zhang, M.; Wang, F.; Pan, C.; Wang, P. Efficient Dye-Sensitized Solar Cells with an Organic Photosensitizer Featuring Orderly Conjugated Ethylenedioxythiophene and Dithienosilole Blocks. *Chem. Mater.* **2010**, *22*, 1915−1925.

(7) Zhang, M.; Wang, Y.; Xu, M.; Ma, W.; Li, R.; Wang, P. Design of High-Efficiency Organic Dyes for Titania Solar Cells Based on the Chromophoric Core of Cyclopentadithiophene-Benzothiadiazole. *Energy Environ. Sci.* **2013**, *6*, 2944−2949.

(8) Yum, J.-H.; Hagberg, D. P.; Moon, S.-J.; Karlsson, K. M.; Marinado, T.; Sun, L.; Hagfeldt, A.; Nazeeruddin, M. K.; Grätzel, M. A Light-Resistant Organic Sensitizer for Solar-Cell Applications. *Angew. Chem., Int. Ed.* **2009**, *121*, 1604−1608.

(9) Wu, W.; Zhang, J.; Yang, H.; Jin, B.; Hu, Y.; Hua, J.; Jing, C.; Long, Y.; Tian, H. Narrowing Band Gap of Platinum Acetylide Dye-Sensitized Solar Cell Sensitizers with Thiophene π-Bridges. *J. Mater. Chem.* **2012**, *22*, 5382−5389.

(10) Mizuno, Y.; Yisilamu, Y.; Yamaguchi, T.; Tomura, M.; Funaki, T.; Sugihara, H.; Ono, K. (Dibenzoylmethanato)boron Difluoride Derivatives Containing Triphenylamine Moieties: A New Type of Electron-Donor/π-Acceptor System for Dye-Sensitized Solar Cells. *Chem.—Eur. J.* **2014**, *20*, 13286−13295.

(11) He, J.; Wu, W.; Hua, J.; Jiang, Y.; Qu, S.; Li, J.; Long, Y.; Tian, H. Bithiazole-Bridged Dyes for Dye-Sensitized Solar Cells with High Open Circuit Voltage Performance. *J. Mater. Chem.* **2011**, *21*, 6054−6062.

(12) Michinobu, T.; Satoh, N.; Cai, J.; Lia, Y.; Hanb, L. Novel Design of Organic Donor-Acceptor Dyes without Carboxylic Acid Anchoring Groups for Dye-Sensitized Solar Cells. *J. Mater. Chem. C* **2014**, *2*, 3367−3372.

(13) Khanasa, T.; Jantasing, N.; Morada, S.; Leesakul, N.; Tarsang, R.; Namuangruk, S.; Kaewin, T.; Jungsuttiwong, S.; Sudyoadsuk, T.; Promarak, V. Synthesis and Characterization of 2D-D-π-A-Type Organic Dyes Bearing Bis(3,6-di-*tert*-butylcarbazol-9-ylphenyl)aniline as Donor Moiety for Dye-Sensitized Solar Cells. *Eur. J. Org. Chem.* **2013**, 2608−2620.

(14) Horiuchi, T.; Miura, H.; Sumioka, K.; Uchida, S. High Efficiency of Dye-Sensitized Solar Cells Based on Metal-Free Indoline Dyes. *J. Am. Chem. Soc.* **2004**, *126*, 12218−12219.

(15) Higashijima, S.; Inoue, Y.; Miura, H.; Kubota, Y.; Funabiki, K.; Yoshida, T.; Matsui, M. Organic Dyes Containing Fluorene-Substituted Indoline Core for Zinc Oxide Dye-Sensitized Solar Cell. *RSC Adv.* **2012**, *2*, 2721−2724.

(16) Koumura, N.; Wang, Z.-S.; Miyashita, M.; Uemura, Y.; Sekiguchi, H.; Cui, Y.; Mori, A.; Mori, S.; Hara, K. Substituted Carbazole Dyes for Efficient Molecular Photovoltaics: Long Electron Lifetime and High Open Circuit Voltage Performance. *J. Mater. Chem.* **2009**, *19*, 4829−4836.

(17) Su, J.-Y.; Lo, C.-Y.; Tsai, C.-H.; Chen, C.-H.; Chou, S.-H.; Liu, S.-H.; Chou, P.-T.; Wong, K.-T. Indolo[2,3-*b*]carbazole Synthesized from a Double-Intramolecular Buchwald-Hartwig Reaction: Its Application for a Dianchor DSSC Organic Dye. *Org. Lett.* **2014**, *16*, 3176−3179.

(18) Luo, C.; Bi, W.; Deng, S.; Zhang, J.; Chen, S.; Li, B.; Liu, Q.; Peng, H.; Chu, J. Indolo[3,2,1-jk]carbazole Derivatives-Sensitized Solar Cells: Effect of π-Bridges on the Performance of Cells. *J. Phys. Chem. C* **2014**, *118*, 14211−14217.

(19) Murakami, T. N.; Koumura, N.; Kimura, M.; Mori, S. Structural Effect of Donor in Organic Dye on Recombination in Dye-Sensitized Solar Cells with Cobalt Complex Electrolyte. *Langmuir* **2014**, *30*, 2274−2279.

(20) Jo, H. J.; Nam, J. E.; Sim, K.; Kim, D.-H.; Kim, J. H.; Kang, J.-K. Molecular Design and Photovoltaic Performance of Organic Dyes Containing Phenothiazine for Dye-Sensitized Solar Cells. *J. Nanosci. Nanotechnol.* **2014**, *14*, 7938−7942.

(21) Funabiki, K.; Mase, H.; Hibino, A.; Tanaka, N.; Mizuhata, N.; Sakuragi, Y.; Nakashima, A.; Yoshida, T.; Kubotaa, Y.; Matsuia, M. Synthesis of a Novel Heptamethine-Cyanine Dye for Use in near-Infrared Active Dye-Sensitized Solar Cells with Porous Zinc Oxide Prepared at Low Temperature. *Energy Environ. Sci.* **2011**, *4*, 2186−2192.

(22) Wu, W.; Guo, F.; Li, J.; He, J.; Hua, J. New Fluoranthene-based Cyanine Dye for Dye-Sensitized Solar Cells. *Synth. Met.* **2010**, *160*, 1008−1014.

(23) Tang, J.; Wu, W.; Hua, J.; Li, J.; Li, X.; Tian, H. Starburst Triphenylamine-based Cyanine Dye for Efficient Quasi-Solid-State Dye-Sensitized Solar Cells. *Energy Environ. Sci.* **2009**, *2*, 982−990.

(24) Wang, J.; Li, M.; Qi, D.; Shen, W.; He, R.; Lin, S. H. Exploring Photophysical Properties of Metal-Free Coumarin Sensitizers: An Efficient Strategy to Improve the Performance of Dye-Sensitized Solar Cells. *RSC Adv.* **2014**, *4*, 53927−53938.

(25) Wang, Z.-S.; Cui, Y.; Hara, K.; Dan-oh, Y.; Kasada, C.; Shinpo, A. A High-Light-Harvesting-Efficiency Coumarin Dye for Stable Dye-Sensitized Solar Cells. *Adv. Mater.* **2007**, *19*, 1138−1141.

(26) Seo, K. D.; Choi, I. T.; Park, Y. G.; Kang, S.; Lee, J. Y.; Kim, H. K. Novel D-A-π-A Coumarin Dyes Containing Low Band-Gap Chromophores for Dye-Sensitised Solar Cells. *Dyes Pigm.* **2012**, *94*, 469−474.

(27) Venkatraman, V.; Alsberg, B. K. A Quantitative Structure-Property Relationship Study of the Photovoltaic Performance of Phenothiazine Dyes. *Dyes Pigm.* **2015**, *114*, 69−77.

(28) Hua, Y.; Chang, S.; He, J.; Zhang, C.; Zhao, J.; Chen, T.; Wong, W. Y.; Wong, W.-K.; Zhu, X. Molecular Engineering of Simple Phenothiazine-Based Dyes To Modulate Dye Aggregation, Charge Recombination, and Dye Regeneration in Highly Efficient Dye-Sensitized Solar Cells. *Chem.—Eur. J.* **2014**, *20*, 6300−6308.

DOI: 10.1021/acsami.5b03783
ACS Appl. Mater. Interfaces 2015, 7, 14975−14982

(29) Wu, W.; Yang, J.; Hua, J.; Tang, J.; Zhang, L.; Long, Y.; Tian, H. Efficient and Stable Dye-Sensitized Solar Cells Based on Phenothiazine Sensitizers with Thiophene Units. *J. Mater. Chem.* **2010**, *20*, 1772−1779.
(30) Sun, X.; Wang, Y.; Li, X.; Ågren, H.; Zhu, W.; Tiana, H.; Xie, Y. Cosensitizers for Simultaneous Filling Up of Both Absorption Valleys of Porphyrins: A Novel Approach for Developing Efficient Panchromatic Dye-Sensitized Solar Cells. *Chem. Commun.* **2014**, *50*, 15609−15612.
(31) Chen, C.; Yang, X.; Cheng, M.; Zhang, F.; Sun, L. Degradation of Cyanoacrylic Acid-based Organic Sensitizers in Dye-Sensitized Solar Cells. *ChemSusChem* **2013**, *6*, 1270−1275.
(32) Zietz, B.; Gabrielsson, E.; Johansson, V.; El-Zohry, A. M.; Sun, L.; Kloo, L. Photoisomerization of the Cyanoacrylic Acid Acceptor Group - A Potential Problem for Organic Dyes in Solar Cells. *Phys. Chem. Chem. Phys.* **2014**, *16*, 2251−2255.
(33) Ooyama, Y.; Inoue, S.; Nagano, T.; Kushimoto, K.; Ohshita, J.; Imae, I.; Komaguchi, K.; Harima, Y. Dye-Sensitized Solar Cells Based on Donor-Acceptor π-Conjugated Fluorescent Dyes with a Pyridine Ring as an Electron-Withdrawing Anchoring Group. *Angew. Chem., Int. Ed.* **2011**, *123*, 7567−7571.
(34) Ooyama, Y.; Yamaguchi, N.; Imae, I.; Komaguchi, K.; Ohshita, J.; Harima, Y. Dye-Sensitized Solar Cells Based on D-π-A Fluorescent Dyes with Two Pyridyl Groups as an Electron-Withdrawing-Injecting Anchoring Group. *Chem. Commun.* **2013**, *49*, 2548−2550.
(35) López-Duarte, I.; Wang, M.; Humphry-Baker, R.; Ince, M.; Martínez-Díaz, M. V.; Nazeeruddin, M. K.; Torres, T.; Grätzel, M. Molecular Engineering of Zinc Phthalocyanines with Phosphinic Acid Anchoring Groups. *Angew. Chem., Int. Ed.* **2012**, *124*, 1931−1934.
(36) He, H.; Gurung, A.; Si, L. 8-Hydroxylquinoline as a Strong Alternative Anchoring Group for Porphyrin-Sensitized Solar Cells. *Chem. Commun.* **2012**, *48*, 5910−5912.
(37) Cheng, M.; Yang, X.; Li, J.; Chen, C.; Zhao, J.; Wang, Y.; Sun, L. Dye-Sensitized Solar Cells Based on a Donor-Acceptor System with a Pyridine Cation as an Electron-Withdrawing Anchoring Group. *Chem.—Eur. J.* **2012**, *18*, 16196−16202.
(38) Zhao, J.; Yang, X.; Cheng, M.; Li, S.; Sun, L. Molecular Design and Performance of Hydroxylpyridium Sensitizers for Dye-Sensitized Solar Cells. *ACS Appl. Mater. Interfaces* **2013**, *5*, 5227−5231.
(39) Mao, J.; He, N.; Ning, Z.; Zhang, Q.; Guo, F.; Chen, L.; Wu, W.; Hua, J.; Tian, H. Stable Dyes Containing Double Acceptors without COOH as Anchors for Highly Efficient Dye-Sensitized Solar Cells. *Angew. Chem., Int. Ed.* **2012**, *124*, 10011−10014.
(40) Ooyama, Y.; Hagiwara, Y.; Mizumo, T.; Harima, Y.; Ohshita, J. Photovoltaic Performance of Dye-Sensitized Solar Cells Based on D-π-A Type BODIPY Dye with Two Pyridyl Groups. *New J. Chem.* **2013**, *37*, 2479−2485.
(41) Ooyama, Y.; Nagano, T.; Inoue, S.; Imae, I.; Komaguchi, K.; Ohshita, J.; Harima, Y. Dye-Sensitized Solar Cells Based on Donor-π-Acceptor Fluorescent Dyes with a Pyridine Ring as an Electron-Withdrawing-Injecting Anchoring Group. *Chem.—Eur. J.* **2011**, *17*, 14837−14843.
(42) Cecconi, B.; Mordini, A.; Reginato, G.; Za-ni, L.; Taddei, M.; Fabrizi de Biani, F.; De Angelis, F.; Marotta, G.; Salvatori, P.; Calamante, M. Pyridine-*N*-oxide 2-Carboxylic Acid: An Acceptor Group for Organic Sensitizers with Enhanced Anchoring Stability in Dye-Sensitized Solar Cells. *Asian J. Org. Chem.* **2014**, *3*, 140−152.
(43) Wu, C.-H.; Chen, M.-C.; Su, P.-C.; Kuo, H.-H.; Wang, C.-L.; Lu, C.-Y.; Tsai, C.-H.; Wu, C.-C.; Lin, C.-Y. Porphyrins for Efficient Dye-Sensitized Solar Cells Covering the near-IR Region. *J. Mater. Chem. A* **2014**, *2*, 991−999.
(44) Wang, C.-L.; Lan, C.-M.; Hong, S.-H.; Wang, Y.-F.; Pan, T.-Y.; Chang, C.-W.; Kuo, H.-H.; Kuo, M.-Y.; Diau, E. W.-G.; Lin, C.-Y. Enveloping Porphyrins for Efficient Dye-Sensitized Solar Cells. *Energy Environ. Sci.* **2012**, *5*, 6933−6940.
(45) Wang, C.-L.; Chang, Y.-C.; Lan, C.-M.; Lo, C.-F.; Diau, E. W.-G.; Lin, C.-Y. Enhanced Light Harvesting with π-Conjugated Cyclic Aromatic Hydrocarbons for Porphyrin-Sensitized Solar Cells. *Energy Environ. Sci.* **2011**, *4*, 1788−1795.
(46) Luo, J.; Xu, M.; Li, R.; Huang, K.-W.; Jiang, C.; Qi, Q.; Zeng, W.; Zhang, J.; Chi, C.; Wang, P. J. Wu. *N*-Annulated Perylene as an Efficient Electron Donor for Porphyrin-based Dyes: Enhanced Light-Harvesting Ability and High-Efficiency Co(II/III)-based Dye-Sensitized Solar Cells. *J. Am. Chem. Soc.* **2014**, *136*, 265−272.
(47) Yella, A.; Lee, H.-W.; Tsao, H. N.; Yi, C.; Chandiran, A. K.; Nazeeruddin, M. K.; Diau, E. W.-G.; Yeh, C.-Y.; Zakeeruddin, S. M.; Grätzel, M. Porphyrin-Sensitized Solar Cells with Cobalt (II/III)-based Redox Electrolyte Exceed 12% Efficiency. *Science* **2011**, *334*, 629−634.
(48) Mathew, S.; Yella, A.; Gao, P.; Humphry-Baker, R.; Curchod, B. F. E.; Ashari-Astani, N.; Tavernelli, I.; Rothlisberger, U.; Nazeeruddin, M. K.; Grätzel, M. Dye-Sensitized Solar Cells with 13% Efficiency Achieved through the Molecular Engineering of Porphyrin Sensitizers. *Nat. Chem.* **2014**, *6*, 242−247.
(49) Yella, A.; Mai, C.-L.; Zakeeruddin, S. M.; Chang, S.-N.; Hsieh, C.-H.; Yeh, C.-Y.; Grätzel, M. Molecular Engineering of Push-Pull Porphyrin Dyes for Highly Efficient Dye-Sensitized Solar Cells: The Role of Benzene Spacers. *Angew. Chem., Int. Ed.* **2014**, *126*, 3017−3021.
(50) Zhao, J.; Yang, X.; Cheng, M.; Li, S.; Sun, L. Molecular Design and Performance of Hydroxylpyridium Sensitizers for Dye-Sensitized Solar Cells. *ACS Appl. Mater. Interfaces* **2013**, *5*, 5227−5231.
(51) Lin, L. Y.; Tsai, C. H.; Wong, K. T.; Huang, T. W.; Hsieh, L.; Liu, S. H.; Lin, H. W.; Wu, C. C.; Chou, S. H.; Chen, S. H.; Tsai, A. I. Organic Dyes Containing Coplanar Diphenyl-Substituted Dithienosilole Core for Efficient Dye-Sensitized Solar Cells. *J. Org. Chem.* **2010**, *75*, 4778−4785.
(52) Klein, C.; Nazeeruddin, M. K.; Censo, D. D.; Liska, P.; Grätzel, M. Amphiphilic Ruthenium Sensitizers and Their Applications in Dye-Sensitized Solar Cells. *Inorg. Chem.* **2004**, *43*, 4216−4226.
(53) Hagberg, D. P.; Yum, J.-H.; Lee, H.; De Angelis, F.; Marinado, T.; Karlsson, K. M.; Humphry-Baker, R.; Sun, L.; Hagfeldt, A.; Grätzel, M.; Nazeeruddin, K. M. Molecular Engineering of Organic Sensitizers for Dye-Sensitized Solar Cell Applications. *J. Am. Chem. Soc.* **2008**, *130*, 6259−6266.
(54) Park, J. K.; Lee, H. R.; Chen, J.; Shinokubo, H.; Osuka, A.; Kim, D. Photoelectrochemical Properties of Doubly β-Functionalized Porphyrin Sensitizers for Dye-Sensitized Nanocrystalline-TiO_2 Solar Cells. *J. Phys. Chem. C* **2008**, *112*, 16691−16699.
(55) Hagberg, D. P.; Edvinsson, T.; Marinado, T.; Boschloo, G.; Hagfeldt, A.; Sun, L. A Novel Organic Chromophore for Dye-Sensitized Nanostructured Solar Cells. *Chem. Commun.* **2006**, 2245−2247.

DOI: 10.1021/acsami.5b03783
ACS Appl. Mater. Interfaces 2015, 7, 14975−14982